

Contrail Frequency over the United States from Surface Observations

PATRICK MINNIS

Atmospheric Sciences Research, NASA Langley Research Center, Hampton, Virginia

J. KIRK AYERS AND MICHELE L. NORDEEN

AS&M, Inc., Hampton, Virginia

STEVEN P. WEAVER

88th Weather Squadron, Wright-Patterson AFB, Ohio

(Manuscript received 12 August 2002, in final form 10 March 2003)

ABSTRACT

Contrails have the potential for affecting climate because they impact the radiation budget and the vertical distribution of moisture. Estimating the effect requires additional knowledge about the temporal and spatial variations of contrails. The mean hourly, monthly, and annual frequencies of daytime contrail occurrence are estimated using 2 yr of observations from surface observers at military installations scattered over the continental United States. During both years, persistent contrails are most prevalent in the winter and early spring and are seen least often during the summer. They co-occur with cirrus clouds 85% of the time. The annual mean persistent contrail frequencies in unobscured skies dropped from 0.152 during 1993–94 to 0.124 in 1998–99 despite a rise in air traffic. Mean hourly contrail frequencies reflect the pattern of commercial air traffic, with a rapid increase from sunrise to midmorning followed by a very gradual decrease during the remaining daylight hours. Although highly correlated with air traffic fuel use, contrail occurrence is governed by meteorological conditions. It is negatively and positively correlated with the monthly mean 300-hPa temperature and 300-hPa relative humidity, respectively, from the National Centers for Environmental Prediction (NCEP) reanalyses. A simple empirical model employing the fuel use and the monthly mean 300-hPa temperatures and relative humidities yields a reasonable representation of the seasonal variation in contrail frequency. The interannual drop in contrail frequency coincides with a decrease in mean 300-hPa relative humidities from 45.8% during the first period to 38.2% in 1998–99, one of the driest periods in the NCEP record.

1. Introduction

Contrails are a common sight in the skies over the United States and Europe. They represent a change in atmospheric composition that may impact climate because, as a type of cirrus cloud, they affect the earth radiation budget by reflecting and absorbing solar radiation and emitting and absorbing infrared radiation (e.g., Minnis et al. 1999; Ponater et al. 2002). They may also redistribute upper-tropospheric moisture through sedimentation (Penner et al. 1999). In a recent assessment (Penner et al. 1999), contrails and their effects were recognized as one of the largest outstanding uncertainties in the air traffic impact on the atmosphere. Contrail coverage, distribution, and optical depth are some of the variables that must be accurately quantified. With commercial jet air traffic expected to continue in-

creasing at a rate of 2%–5% per annum through 2050 (Penner et al. 1999), it is important to reduce the uncertainties in the parameters that determine the impact of contrails on climate.

The locations of the contrails and the month and time of day when they form affect how they interact with the radiation field (Meerkötter et al. 1999). Satellite estimates of contrail coverage (Bakan et al. 1994; Mannstein et al. 1999; DeGrand et al. 2000) provide the only empirical information for estimating contrail distribution and coverage, while models using numerical weather analyses can provide theoretical estimates of contrail coverage (e.g., Sausen et al. 1998; Duda et al. 2002). Satellite estimates are prone to uncertainty because of differences in analysis techniques, satellite sensor differences, and difficulties in discriminating contrails from natural cloud formations. Theoretical results are also subject to large uncertainties for a variety of reasons including the lack of detailed, accurate upper-tropospheric humidity data (Miloshevich et al. 2001; Minnis et al. 2002) and difficulties in modeling contrails as

Corresponding author address: Patrick Minnis, NASA Langley Research Center, MS 420, Hampton, VA 23681-0001.
E-mail: p.minnis@nasa.gov

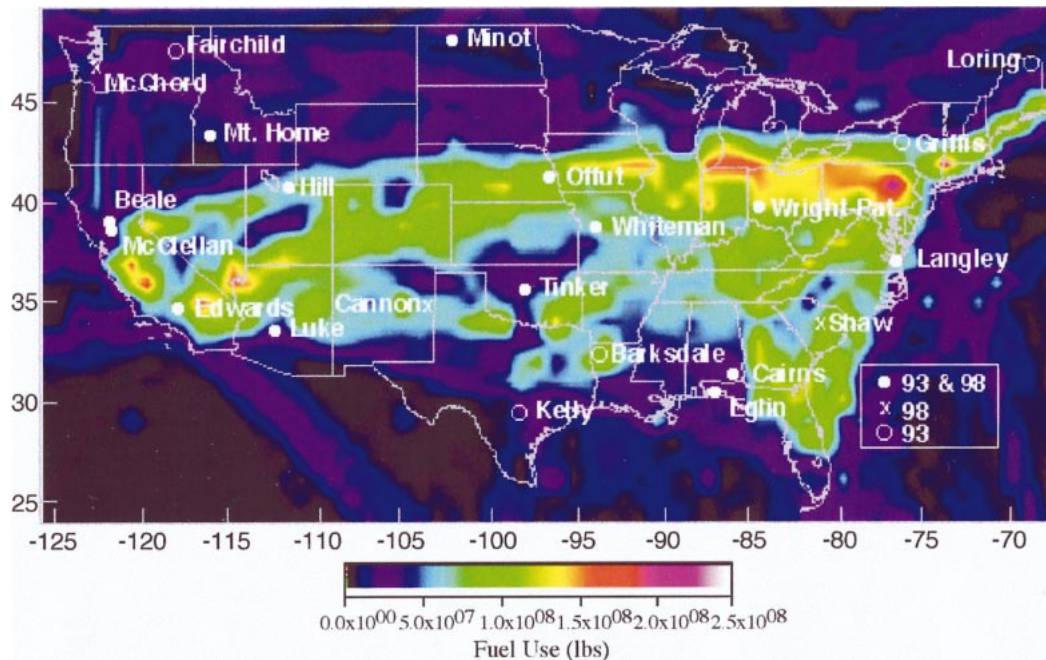


FIG. 1. Contrail observing sites for the two periods overlaying the fuel use estimate for May 1990.

quantities distinct from natural cirrus clouds (Ponater et al. 2002). An independent means of quantifying contrails is needed to help validate and assess both the model and satellite estimates of contrail distributions.

Minnis et al. (1997) documented the frequency of contrail occurrence over the United States based on a year of hourly surface observations taken at U.S. Air Force (USAF) bases (AFBs) during 1993–94. They found a distinctive seasonal cycle and diurnal variations of contrail occurrence that were related to jet traffic patterns. Their results are based on a single year of data and may not represent the climatological variability of contrail occurrence over the United States. To establish a more reliable climatology of contrail frequencies and gain a better understanding of their variability, contrail observations were taken for an additional year at USAF bases during 1998–99. These more recent observations are analyzed here and compared and combined with the data taken during 1993–94 to establish a more reliable contrail occurrence climatology for the contiguous United States. The results should be valuable for better understanding of contrail spatial and temporal variability and for validating model calculations and satellite observations.

2. Data

a. Contrail frequency

The raw data were taken by weather observers at USAF or Army airfields distributed over the continental United States (CONUS) as shown in Fig. 1 for the first and second periods. The coordinates and number of

sampled months for each site are given in the appendix. Nominally, an observation was taken once each hour every day at 19 bases during the first period (January 1993–May 1994) and at 17 bases during the second observing period (March 1998–March 1999). The actual monthly coverage varied with station. The geographical distribution changed from the first to the second periods because of base closings, reduction in airfield operating hours, and availability of observers. Fewer months were sampled during the second period than during the first period. During 1993–94, observations were taken during 94% of the possible time slots compared with only 75% for 1998–99. Data were taken at only 31% and 44% of the sites during March and February 1999 and up to 94% during April 1998. Observations during the second period ranged from only 1 month at Whiteman AFB to 12 months at Beale, McChord, Shaw, and Tinker AFBs (specific locations are given in Table A1). Since these are daytime data, the number of samples per day varied with season.

Each observation is classified into one of four categories: no contrails, nonpersistent contrails, persistent contrails (PCs), and obscured. Additionally, each classification was qualified as being with or without cirrus. Finally, the contrail observations were not always taken resulting in a no-observation category. The obscured category is a result of thick haze or clouds blocking the view of the observer to the upper troposphere. A non-persistent or short-lived contrail is defined as one that tends to evaporate and extends only a short distance from the aircraft. A PC extends at least several miles behind the aircraft, shows no dissipation during the ob-

servational time, and appears to spread. Older PCs that have spread and cannot be linked to an aircraft were recorded as contrails when they could be identified. Older contrails can develop into cirrus clouds that are unrecognizable as contrails (Minnis et al. 1998). Thus, these estimates might underreport PC occurrence.

Monthly and hourly means were computed to determine the seasonal and diurnal (as opposed to nocturnal) variations of these categories for each site. The same statistics were also computed with obscured data excluded. These latter results, which implicitly assume that the contrail probabilities are the same in normal and obscured conditions, might be more representative of the true frequencies of contrail occurrence. Minnis et al. (1997) provide a detailed description of the data, sampling, and averaging procedures. Due to reduced sampling during 1998–99, averages were also computed separately for the 13 sites using only those months that were common to both periods for each site.

b. Air traffic data

The air traffic information consists of the May 1990 fuel use estimates f above 7 km on a 1° latitude–longitude grid (Baughcum et al. 1993) that were used for analysis of the 1993–94 contrail data (Minnis et al. 1997). The May 1990 data are used to represent the annual mean fuel use (see Fig. 1). The mean fuel use for each month f_m was estimated by adjusting f by the monthly percent deviation of NO_x emissions from the annual mean over North America between 9 and 13 km from Figs. 2–3 of Baughcum (1996). The NO_x emission is directly proportional to the fuel burned. Between 1994 and 1997, it is estimated that the air traffic increased at a rate of roughly $5\% \text{ yr}^{-1}$ over the CONUS [the International Civil Aviation Organization (ICAO) 1998]. Thus, the fuel usage should have increased by 28% from 1993 to 1998. For correlation with the 1998–99 observations, the May 1990 dataset was uniformly increased by 28% using the assumption that traffic patterns did not change substantially during the interim. For each site, a value of f_m was computed by averaging the fuel use for a 3° box centered on the 1° region containing the site.

c. Temperature and humidity

Contrails form when the relative humidity Rh with respect to water exceeds 100% in the exhaust plume of the aircraft and the temperature T is less than about -39°C . They will persist and spread when the relative humidity with respect to ice Rhi in the ambient air exceeds 100%. Ideally, it would be desirable to know the value of Rh and T for each contrail observation. However, radiosonde profiles of Rh and T over the CONUS are geographically sparse, available only at 0000 and 1200 UTC, and temporally inconsistent because of changes in sensors, recording practices, and data-re-

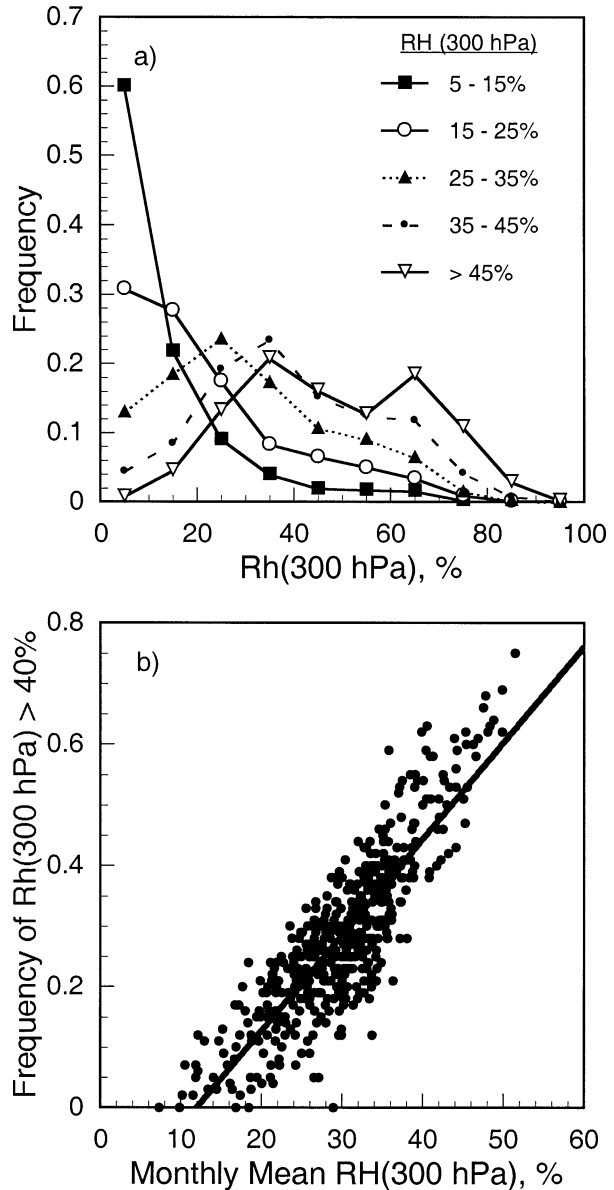


FIG. 2. Statistics of 300-hPa relative humidities from radiosonde data taken near observing sites during 1993–94 and 1998–99. (a) Probability distribution of instantaneous relative humidity as a function monthly mean relative humidity and (b) correlation between the frequency of relative humidity and monthly mean relative humidity.

duction procedures (e.g., Elliott et al. 1998). The conditions that support contrail formation conditions may only last for a few hours over a given location and 12-hourly profiles would be inadequate for accurately assessing the contrail potential at a given time and place. Furthermore, the altitude of a contrail observed from the surface is unknown. The monthly mean relative humidities Rh and temperatures T at 300 hPa (the greatest altitude with humidity data) from the National Centers for Environmental Prediction–National Center for Atmospheric Research (NCEP–NCAR) reanalyses (Kistler

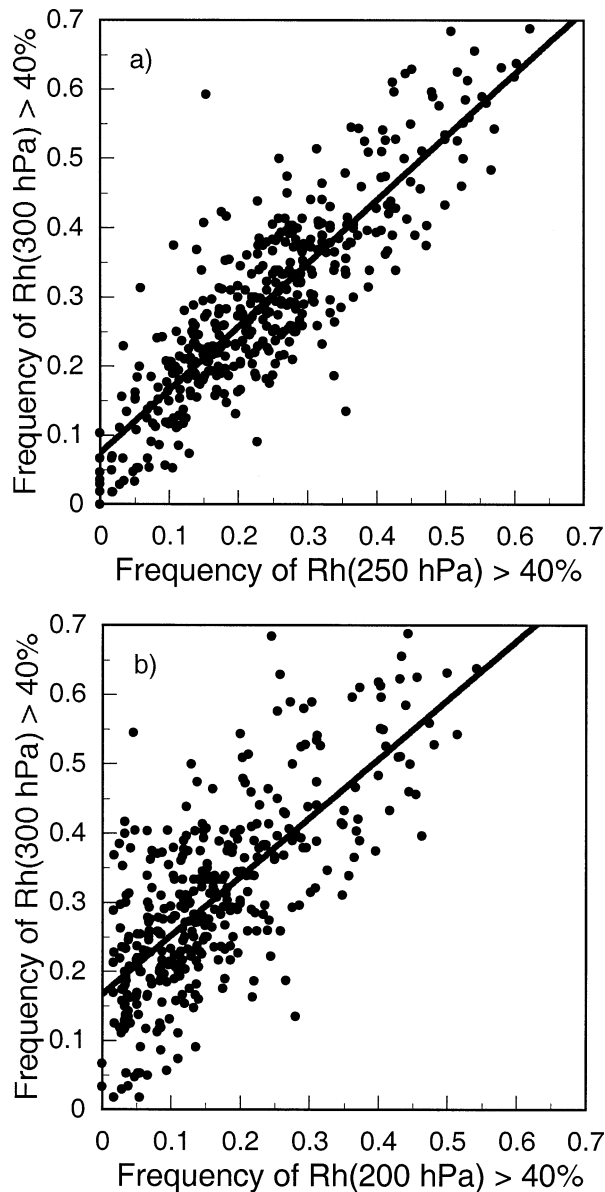


FIG. 3. Correlations of monthly frequency of 300-hPa relative humidities greater than 40% from radiosonde data taken near observing sites during 1993–94 and 1998–99 with corresponding frequency of relative humidities greater than 40% at (a) 250 and (b) 200 hPa.

et al. 2001) on a 2.5° grid were used as a proxy for detailed assessment of the meteorological conditions at each location. The values from the 2.5° region that encompasses a given surface site were merged with the corresponding contrail results. While it is recognized that the NCEP values are not perfect, they should be more temporally and spatially consistent than the radiosonde data because of the physical constraints of the model used for the reanalysis. In addition, they provide values over any location in the United States. As shown below, the monthly means at 300 hPa provide a rea-

sonable measure of the probability for contrail formation in an average sense.

To a first approximation, persistent contrails should develop when $Rh_i > 100\%$ and $T < -39^\circ\text{C}$. However, Rh is the quantity typically available from model or radiosonde data. Nominally, the value of Rh corresponding to $Rh_i = 100\%$ decreases almost linearly from 76% at -30°C to 52% at -70°C (e.g., Sassen 1997). The radiosondes used in the United States typically measure humidity (Gaffen 1993) with a carbon hygrometer (e.g., VIZ-B) or a capacitive thin film element (e.g., Vaisala RS-80A). Both sensor types yield similar dry biases in upper-tropospheric humidity (UTH) compared to satellite measurements (Soden and Lanzante 1996). Using comparisons of Vaisala RS-80A and frost-point hygrometer data, Miloshevich et al. (2001) developed an empirical correction factor that, when applied to the Vaisala RS-80A profiles, would yield actual ice-saturation values of Rh that vary from 62% at -30°C to 22% at -70°C . Similar results would be expected for the VIZ-B sensors. The frequency of occurrence of Rh exceeding ice saturation at cold temperatures should be a good measure of the potential for contrail formation. This frequency for a given month should be related to the monthly mean relative humidity $RH(p)$ at pressure p .

To examine this assumption, histograms of the frequency of Rh at 300 hPa were computed for different ranges of $RH(300\text{ hPa})$ using radiosonde profiles taken at the National Weather Service station nearest each AFB surface site within a radius of 300 km during 1993, 1994, 1998, and 1999. Radiosondes from a total of 12 stations were used. The maxima in the probability distributions in Fig. 2a shift from 5% for $RH < 15\%$ to 35% for $RH > 45\%$, the range with a secondary maximum at $Rh = 65\%$. The frequencies of Rh between 40% and 50% are nearly identical for the last two RH categories. These same data were then used to determine how the frequency of $Rh > 40\%$ varies with RH. This value was selected because $Rh = 40\%$ corresponds to ice saturation at -49°C according to the Miloshevich et al. (2001) correction. Temperatures at 300 hPa reach -49°C mostly during the winter over the CONUS. The data plotted in Fig. 2b yield a linear correlation coefficient $R = 0.86$ between $RH(300\text{ hPa})$ and $Rh > 40\%$. The values of R are 0.93 and 0.75 for $Rh > 30\%$ and 50%, respectively, when correlated with $RH(300\text{ hPa})$. Thus, $RH(300\text{ hPa})$ should be a good measure of the frequency of contrail conditions at 300 hPa when the temperature and a large number of data points are considered.

Most contrails form between 200 and 300 hPa. To ensure that $RH(300\text{ hPa})$ is representative of the conditions for the entire main contrail layer, the frequencies of $Rh > 40\%$ at other pressures were correlated with $RH(300\text{ hPa})$ using the radiosonde data. The results shown in Fig. 3 yield $R = 0.86$ and 0.72 for 250 and 200 hPa, respectively. The correlation for 250 hPa is as strong as that for 300 hPa, while it drops off somewhat

TABLE 1. Annual mean 300-hPa relative humidity over radiosonde sites in the United States near the contrail observing sites.

| Year | Radiosonde RH (%) | NCEP RH (%) |
|------|-------------------|-------------|
| 1993 | 32.0 | 46.9 |
| 1994 | 33.0 | 46.1 |
| 1998 | 28.9 | 39.0 |
| 1999 | 27.9 | 37.3 |

for 200 hPa. While it may not capture all of the scatter and is less representative for 200 than for 250 hPa, RH (300 hPa) should, on average, be a reliable predictor for the mean frequency of potential contrail conditions in the prime contrail layer in the atmosphere.

Finally, because the RH data from NCEP are used instead of those from the radiosonde data, it is necessary to verify that NCEP values are comparable to the available soundings. Monthly means from the NCEP regions containing the radiosonde launch sites were correlated with the corresponding radiosonde monthly means. The correlations are positive for each year with R averaging 0.66 during 1998–99 and only 0.27 during 1993–94, when the radiosonde system was undergoing several changes. Many of the colder ($T < -40^{\circ}\text{C}$) humidity values during 1993 were thrown out in the processing of the radiosonde data (Elliott et al. 1998). Table 1 lists the mean values of RH (300 hPa) for all of the regions together for each year. The NCEP values are 14% and 10% greater than their radiosonde counterparts during 1993–94 and 1998–99, respectively. VIZ-B sondes were primarily used during the earlier period, while Vaisala sondes were scheduled to replace the VIZ-B sondes beginning in 1998. The processing procedures for cold temperature humidities changed dramatically during October 1993 followed by some additional changes in 1997 (Elliott et al. 1998). Thus, the change in the NCEP–radiosonde differences between the two periods is not surprising. The 10% difference during the latter period and, probably, a similar amount during 1993–94, results from an adjustment of the humidity within the NCEP and apparently corrects for much of the dry bias in the observed data. Despite the differences between the two periods, it is clear that the average RH(300 hPa) over these sites decreased significantly in both datasets from 1993–94 to 1998–99.

3. Results

a. Annual means

Figure 4 shows the mean PC frequencies computed relative to the total number of observations and to the number of samples excluding obscured data. The mean values excluding the obscured data range from a minimum of 0.015 at Cairns Army Airfield (AAF) at Ft. Rucker, Alabama, to 0.296 at Wright-Patterson AFB. Data were taken during only four late spring and early fall months at Cairns AAF and are not a particularly

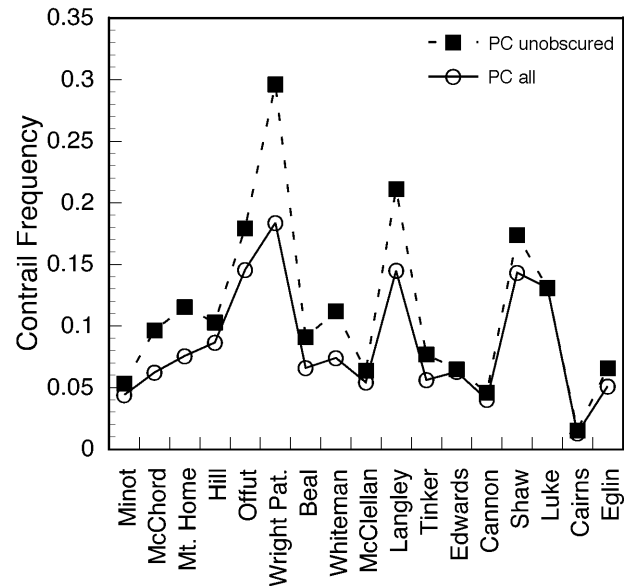


FIG. 4. Mean PC frequencies during 1998–99 observing period for all sites with observations. The sites are ordered from north to south.

good representation of the annual mean. The data from Whiteman AFB were taken during April 1998 only. The maximum value at Wright-Patterson AFB is not surprising given its proximity to the heaviest air traffic area in the country (Fig. 1). Eglin AFB, Cairns AAF, and Minot AFB are generally outside the main airways.

Figure 5 shows the geographical distribution of the annual mean frequencies of PCs without obscured data for both periods. The contrail frequency dropped primarily over the western states during 1998–99, while the average over the east for the second period is comparable to that during 1993–94. The lack of data over the northeastern United States during the second period is readily apparent in these results. Means for stations with fewer than five samples are not shown.

The greatest change between the 1993–94 and 1998–99 datasets occurred at Luke AFB, where the unobscured PC frequency increased from 0.054 to 0.131 in the latter period, a trend opposite that over California. The average site ratios of nonpersistent to persistent contrails during the first and second periods are 0.45 and 0.41, respectively. During 1993–94, this ratio at Luke AFB was 1.7, more than 50% larger than any other site. The ratios exceeded 0.7 at only two other sites for both periods. It is possible that some of the Luke observers classified the PCs improperly during the first period. If it is assumed that the average number of CONUS nonpersistent contrails was observed at Luke AFB during 1993–94, then the average PC frequency for Luke would have to be adjusted upward to account for the assumed and observed number of nonpersistent contrails resulting in a mean value of 0.130 for Luke during 1993–94. This uncertainty should not affect the overall conclu-

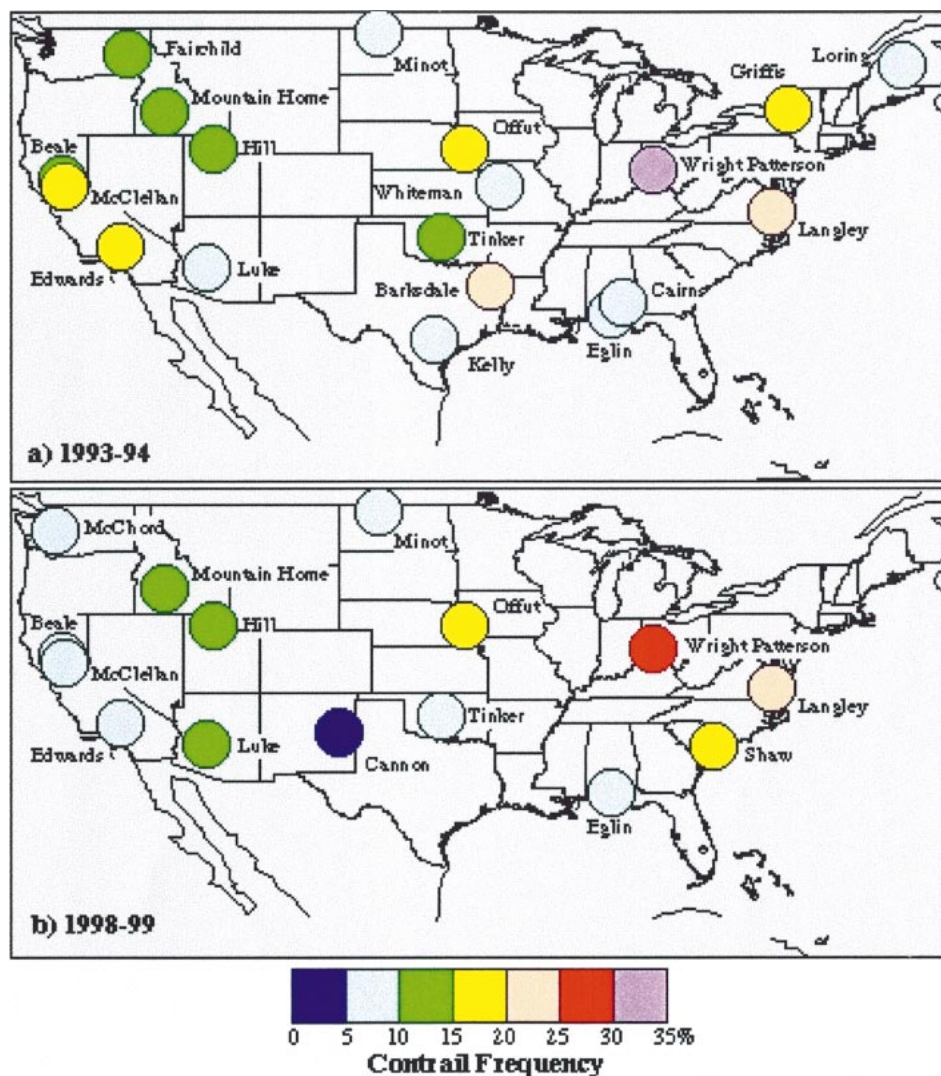


FIG. 5. Annual mean PC frequencies with unobscured data for each site. Sites with fewer than five months of observations are excluded.

sions of this study but would slightly raise the first-period average frequency.

b. Seasonal variations

The 1993–94 and 1998–99 monthly mean PC frequencies are plotted with the standard errors of the mean for each point in Fig. 6. Maximum contrail frequency occurs during February or March for both periods with and without the obscured data. The minimum during the second period occurs in September compared to July during 1993–94. In general, PCs occur least often during summer and most often during winter. The frequencies for the results including all observations in Fig. 6a are statistically the same with means of 0.089 and 0.093 for the first and second periods, respectively.

A straight average of the 1998–99 data without obscured data (Fig. 6b) using the monthly means for each

site is 0.114, a value that is only 75% of the 1993–94 mean of 0.152 (Table 2). This marked difference in the unobscured frequencies is due to a dramatic drop in the number of obscured data during the latter period as seen in Fig. 7. For the considered sites, the skies are completely obstructed most often during winter and least frequently during late summer. The average number of obscured cases was 30.2% and 19.6% during 1993–94 and 1998–99, respectively. The differences in Fig. 6b are statistically significant only during March, April, and September when the contrail frequencies are much greater during the first than during the second period. The relatively large changes in the differences during March and April are due to differences in the occurrence of large frequencies of obscured cases with small contrail frequencies. More sites had large frequencies of both contrails and obscured observations during 1993–94 for those months than during 1998–99. Despite the

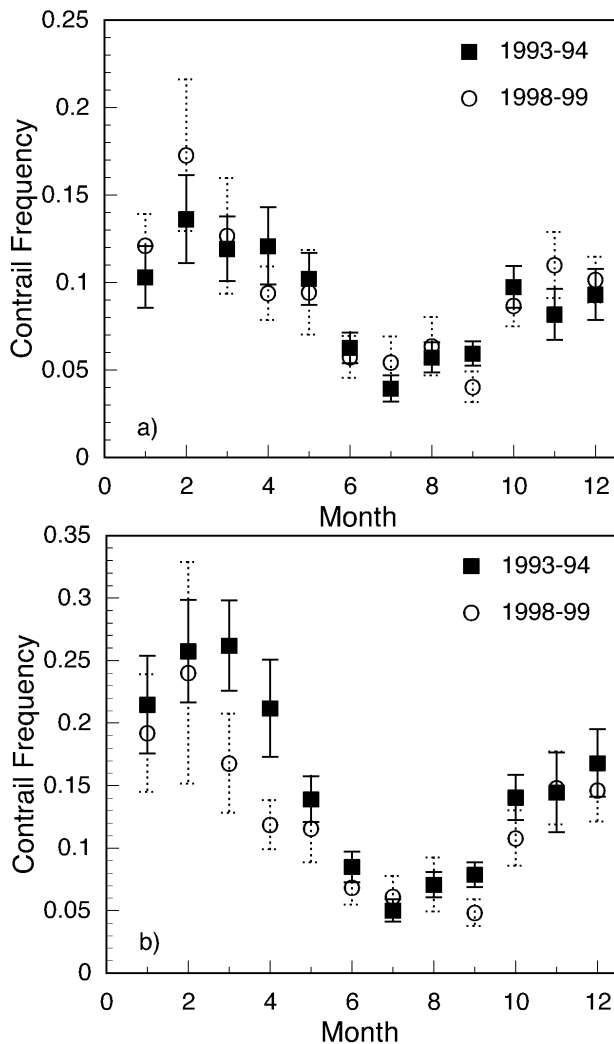


FIG. 6. Monthly mean PC frequencies for both time periods for (a) all data and (b) unobserved data.

greater number of obscured cases during the first period, cirrus clouds were observed simultaneously with PCs 93% of the time during the second period compared to 79% of the time during 1993–94.

Discrepancies in the monthly sampling may also affect the differences between the two observation periods. To examine the impact of sampling differences on

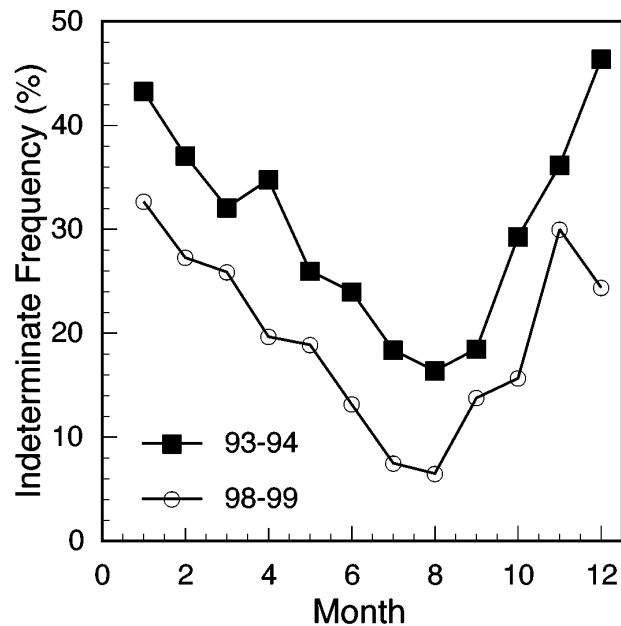


FIG. 7. Monthly mean frequency of obscured data.

the interannual change in PC frequencies, monthly means were computed using unobserved data for the sites and months with observations common to both years. Averages computed using those criteria (Fig. 8), were less in 1998 than during 1993, except for January and July. The seasonal variations are similar to the 1998–99 average. The mean values for the first and second periods in Fig. 8 are 0.134 ± 0.010 and 0.115 ± 0.011 , respectively, which yield a smaller difference, 14%, between the two periods than computed using a straight average of all data. The larger difference based on all of the data is likely due to biased seasonal sampling.

Because of the seasonal similarities between the two datasets, the effects of the nonuniform monthly sampling during 1998–99 on the annual mean can be minimized by using the first period as a guide. An adjusted annual mean value of 0.140 was computed for 1993–94 using the monthly mean PC frequencies without obscured data for the first period weighted by the number of monthly samples for the second period. The ratio of the original 1993–94 mean PC frequency, 0.152, to this

TABLE 2. Contrail frequencies for first and second periods for all sites.

| Parameter | 1993–94 | 1998–99 |
|--|---------|---------|
| Number site months | 234 | 144 |
| Cirrus coincidence (%) | 79 | 93 |
| All PC frequency | 0.089 | 0.093 |
| Unobserved PC frequency | 0.152 | 0.114 |
| Unobserved non-PC frequency | 0.052 | 0.040 |
| Total unobserved contrail frequency | 0.204 | 0.154 |
| Regionally, monthly matched frequency | 0.134 | 0.115 |
| Seasonally normalized, unobserved PC frequency (best estimate) | 0.152 | 0.124 |

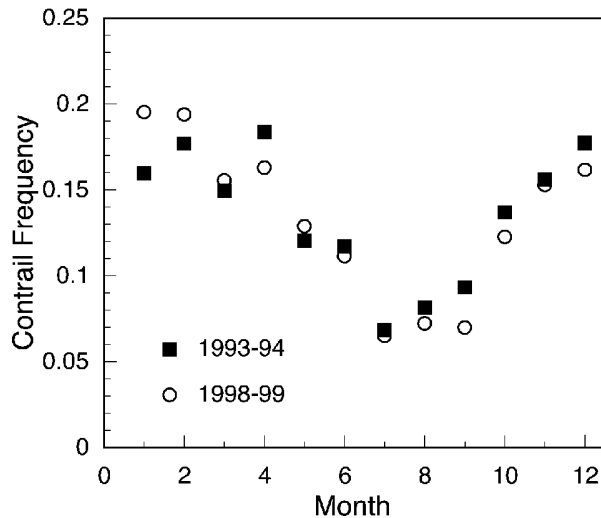


FIG. 8. Monthly mean PC frequencies with unobscured data using only those sites having data during both periods.

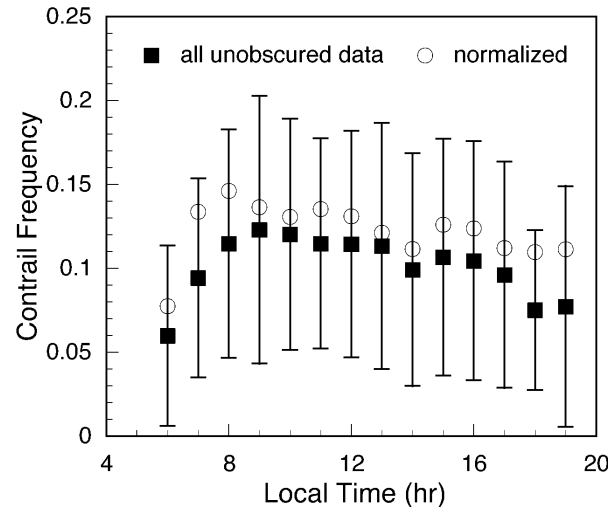


FIG. 9. Mean hourly PC frequency for all regions, 1998–99. Error bars indicate the regional std dev.

adjusted mean provides a seasonal normalization factor of 1.086. Multiplying this factor by the 1998–99 mean yields a seasonally adjusted annual mean for 1998–99 of 0.124. Thus, the true drop in PC frequency between the two periods is probably closer to 18% than the 25% computed using the unadjusted data. The adjusted value is probably more representative of the actual annual mean frequency than the seasonally biased value of 0.114.

Although not climatologically important, short-lived contrails may be of interest for other applications. Non-persistent contrails were seen in 0.040 of the unobscured observations yielding a mean total contrail frequency of 0.154 for all of the sites during 1998–99. This result represents a 24% decrease relative to the short-lived contrails during 1993–94 and is nearly identical to the interannual change in PCs discussed above. The seasonal cycle of short-lived contrails mimics the seasonal variations in the unobscured PCs. Table 2 summarizes the results for all of these different permutations of the dataset.

c. Diurnal cycle

The mean PC frequency (solid symbols) in unobscured conditions is plotted as a function of local time (LT) in Fig. 9. The frequency increases from 0600 to 0900 LT when it peaks at ~ 0.125 and then slowly decreases down to 0.100 by 1700 LT. Persistent contrail occurrence then drops to 0.080 for the remainder of the daylight period. In relative terms, this diurnal variation is nearly identical to that seen in the 1993–94 data (Minnis et al. 1997). The increasing frequencies early in the morning are consistent with the daily cycle of flights that begins around sunrise. Without better flight information, however, it is not clear that the decreased numbers of contrails after 1600 LT are the result of reduced

air traffic or a sampling bias characterized by observations taken only during the summer months when the mean contrail coverage is reduced. To explore this issue, the mean hourly PC frequencies were computed using only those months and sites with averages at all hours between 0600 and 1900 LT. The results, normalized to the seasonally adjusted annual mean, are shown as open symbols in Fig. 9. The peak shifts slightly to 0800 LT and the sudden decrease in the evening disappears indicating that the air traffic remains steady through 1900 LT. The frequency drop seen in the all-unobscured data is apparently due to the seasonal sampling bias that precludes evening observations during autumn and winter.

4. Discussion

a. Unobscured PC versus all-data PC

The difference between the PC occurrences with and without the obscured observations is large. Without the obscured observations, the PC frequency is considerably greater during 1993–94 than during the second period. For model predictions of contrail formation, it is important to determine which dataset more accurately represents the true occurrence over the sites. The statistics of cloud type co-occurrence from the surface cloud observation compilation of Hahn et al. (1984) provide one means for examining this question. Overall, contrails occur in conjunction with cirrus clouds in approximately 85% of PC observations and PCs exist in many of the same conditions that support natural cirrus clouds. Thus, for purposes of co-occurrence with other cloud types, PCs should be similar to the cloud type, cirrus. From the Hahn et al. (1984) summary, the average frequency of cirrus occurrence is 45% for land areas between 30° and 60°N. Hahn et al. (1984) report the frequency of

occurrence of five other distinct cloud types and their co-occurrence frequencies with cirrus and other clouds. The expected frequency of cirrus clouds given the presence of other cloud types is computed by integrating the co-occurrence and occurrence frequencies and dividing by the sum of the occurrence frequencies of the other cloud types. The resulting average co-occurrence frequency of cirrus with any other cloud type is 47%, a value only slightly larger than the average frequency of cirrus. Thus, when lower clouds obscure the sky, it is highly likely that the occurrence of cirrus is the same as when the upper troposphere is not obscured.

It follows that the PC statistics based on the observations without the obscured cases are more representative than those referenced to all observations. The implied random overlap assumption used in the unobscured case is also supported by the study of Tian and Curry (1989) who found that it provides the best estimate of total cloud cover when the cloud layers are separated, a condition that would apply for the distinct layers used by Hahn et al. (1984). Furthermore, they reported that the random overlap assumption is less accurate when the layer cloud amounts are between 30% and 70%, a condition that does not apply to obstructed conditions that define the obscured category.

The frequent occurrence of contrails over extensive lower-level clouds is readily evident in satellite data. For example, the visible channel image (Fig. 10a) from the National Oceanic and Atmospheric Administration Satellite (*NOAA-15*) Advanced Very High Resolution Radiometer (AVHRR) taken at 1303 UTC 3 April 2002 shows extensive area of bright clouds over the south-central United States. Figure 8b is an image created from the brightness temperature difference, $T_4 - T_5$, between AVHRR channels 4 (11 μm) and 5 (12 μm) for the same scene. Younger contrails are often evident as whiter, linear features in $T_4 - T_5$ imagery, which is used for automated contrail detection (e.g., Mannstein et al. 1999). In Fig. 10b, contrails of various ages can be seen to the southwest of points A and B; to the northeast of C; to the north, northwest, and northeast of D; northwest of E; and south, and, possibly, north of point F. With the exception of parts of the contrails near F, all of the contrails would most likely be relegated to the obscured category because of the presence of extensive, optically thick clouds between the surface and the contrails. Shadows cast by the contrails are evident on some of the lower-level clouds. The example satellite image is neither exceptional nor typical; it was selected at random from a publicly available image database maintained at the National Aeronautics and Space Administration (NASA) Langley Research Center (<http://angler.larc.nasa.gov/avhrr/>).

On some days, contrails predominately occur over clear areas and on other days, are seen more frequently over clouds. Given the nature of cloud overlap and the satellite observations, it is concluded that the statistics of PC occurrence without the obscured data are more

representative of the true contrail distribution over the CONUS. Therefore, the results in Fig. 6b showing that contrails were more prevalent during 1993–94 are a more accurate characterization of the seasonal and interannual variations of PC occurrence. Further discussion applies only to the PC statistics without obscured data.

b. Air traffic and temperature dependence

Minnis et al. (1997) showed that the distribution of contrail frequency was related to the aircraft fuel use above 7 km. The relationship between contrail frequency and f is indirect in that different airplanes consume different amounts of fuel and the occurrence of a PC depends on how often and long a plane flies in an environment suitable for contrail formation and persistence. However, such detailed information is currently not available for the time periods under study here and, as noted earlier, the lack of new fuel use data requires the adjustment of the May 1990 dataset (assumed to apply to 1993) to account for 5 yr of air traffic growth between 1993 and 1998. Figure 11 shows the scatterplot and linear least squares regression fit (forced through the origin) between the 1998–99 mean PC frequency of occurrence (adjusted for seasonal bias) C , and f . The two parameters are positively correlated with $R = 0.70$. Although the slope of the line is 30% less than that found for the first period (Minnis et al. 1997), the level of correlation is nearly the same indicating that the patterns have not changed significantly during the interim. The fuel use data explain about half of the spatial variation in annual mean contrail occurrence.

If the original fuel dataset were used in the correlation in Fig. 11, the resulting slope would still be 12% smaller than that for 1993–94 indicating that the change between the two years is significant. The frequency of PC occurrence should have been larger during the second period than during the first if all other factors were equal. The primary parameters determining persistent contrail occurrence are the air traffic density and the flight-level temperature and Rh. As discussed earlier, the NCEP RH (300 hPa), hereafter, simply RH_m , is used as a surrogate for the probability of the occurrence of ice-saturated conditions. Similarly, the monthly mean 300-hPa temperatures T_m are used instead of the instantaneous values. These quantities can be used to determine if the conditions were equivalent during the two periods.

During the first period, RH_m averaged over all of the sites was 45.8% compared to 38.2% during 1998–99. This change is comparable to that for the 12 sites contributing to Table 1. Furthermore, the monthly mean RH_m exceeded 50% in 40.5% of the regional data during 1993–94 compared to 17% during the latter period. Mean temperatures at 300 hPa increased by only 0.5°C between the two periods. Figure 12 shows T_m and RH_m for the matched data used in Fig. 8. The values of RH_m are only comparable for January and February in both

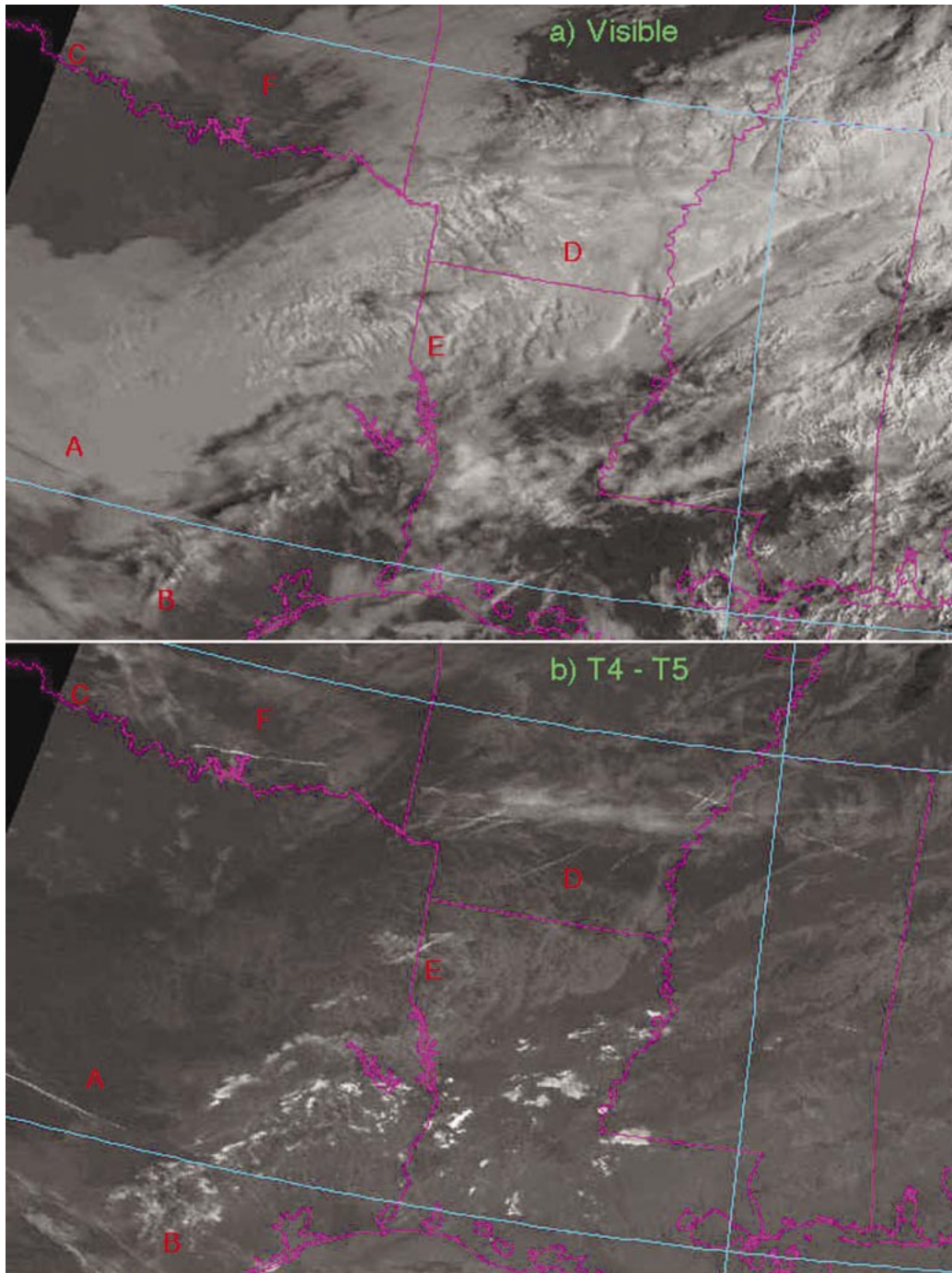


FIG. 10. Imagery from the *NOAA-I5* AVHRR taken 1303 UTC 3 Apr 2002 over the south-central United States.

periods. During the remaining months, RH_m is 5%–11% less during the second period. September 1998 is the driest month at 300 hPa and is 1 K warmer than its first period counterpart. This may explain why the minimum PC frequency occurred in September during the second period. The driest year between 1971 and 2001 at 300 hPa was 1999, while 1998 was the third driest year. The seventh and second wettest years were 1993 and 1994,

respectively, at 300 hPa during that same window. Thus, it is concluded that the conditions favorable for PC formation during the second period were much less likely than for 1993–94 resulting in a decrease in PC frequency, despite an increase in jet air traffic.

The drier upper atmosphere during the second period is also consistent with the decreased number of obscured data in Fig. 7. A drier atmosphere would coincide with

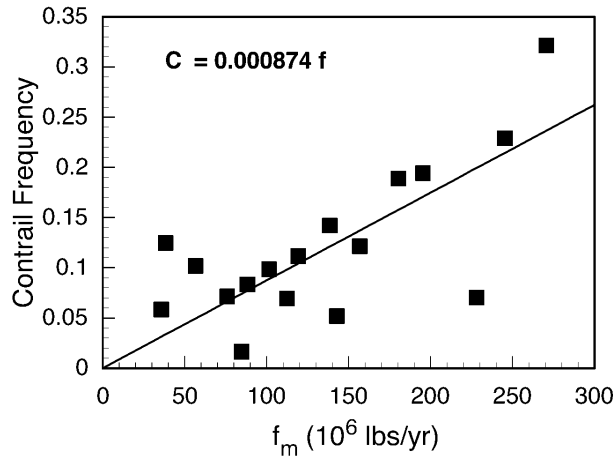


FIG. 11. Correlation of 1998–99 site mean contrail frequencies and estimated fuel use above 7 km.

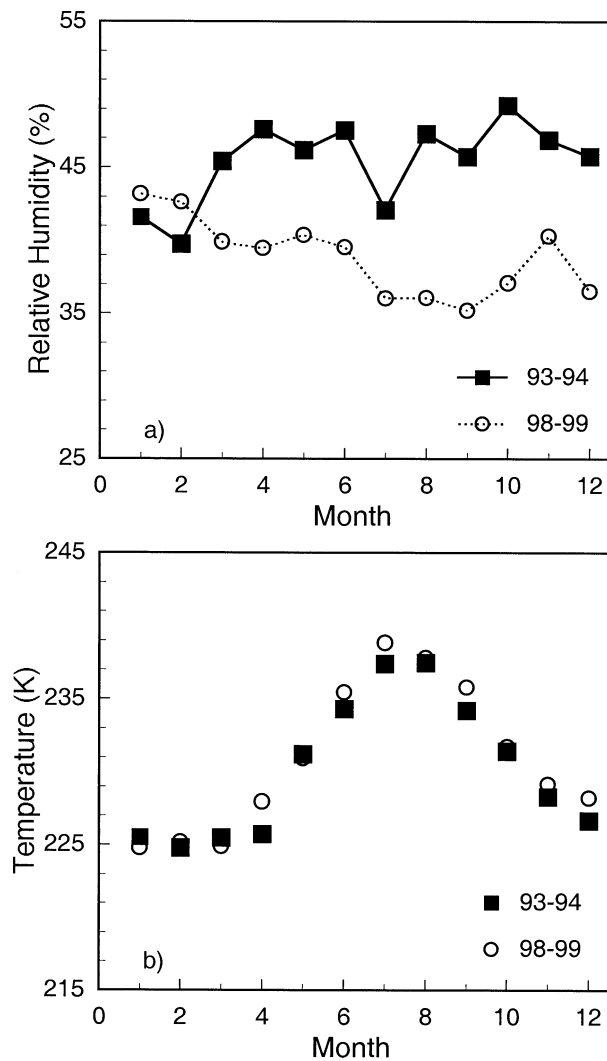


FIG. 12. Monthly mean 300-hPa (a) relative humidities and (b) temperatures for the sites used in Fig. 6.

fewer overcast conditions and less cirrus coverage. The fractional amount of cirrus plus cirrostratus cloud coverage derived from the International Satellite Cloud Climatology Project (ISCCP) dataset (Rossow and Schiffer 1999) over the CONUS dropped from 32.1% for August 1993 through July 1994 to 26.4% during 1998. (The time periods are slightly different from the contrail periods in order to minimize the Mt. Pinatubo eruption effects on the satellite data and because the ISCCP data were only available through the end of 1998 at the time of the analysis.) The seasonal variation of T_m averaged for the domain as a whole is very well correlated with the annual cycle of mean contrail frequencies in Fig. 6b. In this case, $R = 0.88$ confirming that temperature is an extremely important governing factor for contrail formation (e.g., Appleman 1953).

To help explain some of the climatological variations of contrail occurrence, the relationships between the monthly contrail frequency C_m and f_m and the monthly mean temperature T_m and RH_m at 300 hPa are explored in more detail using only those months having data from all sources. Figure 13 shows the correlations and linear regression fits between C_m and f_m (Fig. 13a) and T_m (Fig. 13b) for both periods combined. The linear regression fits:

$$C_m = 0.029 + (0.0023 \times 10^{-6} \text{ lb}^{-1})f_m, \quad \text{and} \quad (1)$$

$$C_m = 1.674 - (0.0067 \text{ K}^{-1})T_m, \quad (2)$$

both produce $R = 0.37$. Forcing the fuel regression line through the origin yields

$$C_m = (0.0101 \times 10^{-6} \text{ lb}^{-1})f_m, \quad (3)$$

which is shown as the heavy line in Fig. 13a. As expected, the slope in (3) is between those derived from the first and second periods separately. According to (2), the contrail frequency is expected to be zero for months with $T_m > 250$ K. If $T_m = 250$ K and the lapse rate is $-6.5^\circ\text{C km}^{-1}$, the mean temperature at 200 hPa would be about -42°C , a value just past the threshold for contrail formation. The monthly mean correlations are noisier than those using the annual mean values (Fig. 11), but they are statistically significant at the 99% confidence level. Fuel and temperature data analyzed separately from each period yield correlations similar to those in Fig. 11. Some of the scatter in the data may be due to the idealized fuel use dataset. Differences in the actual and 1990 flight patterns, will introduce some uncertainty in the fits. The distribution of actual flights above 7.6 km near most of the sites during 10 September 2001 (Palikonda et al. 2002), however, do not appear to be substantially different from Fig. 1 in relative terms. Thus, the error due to a shift in air traffic patterns since the 1990s is probably small.

c. Humidity impact

The RH_m data plotted with C_m in Fig. 14 yield different correlations for each period. For the 1993–94 data

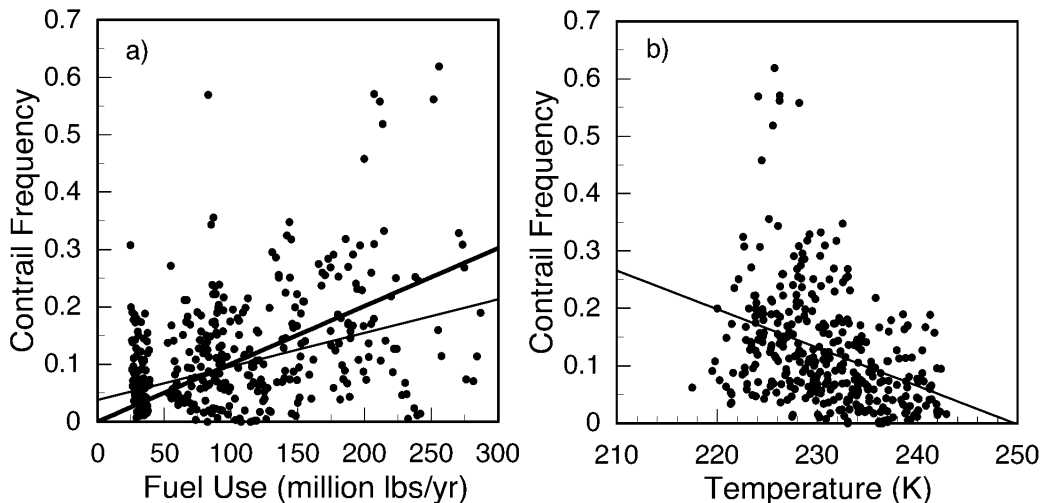


FIG. 13. Correlation of monthly mean contrail frequency and (a) estimated fuel use above 7 km and (b) 300-hPa temperatures. Thin lines indicate linear regression fit. Heavy line indicates regression fit without an intercept.

(Fig. 14a), $R = 0.00$ with no slope in the regression line. The correlation coefficient increases to 0.33 for 1998–99 (Fig. 14b) yielding the regression line:

$$C_m = -0.062 + 0.0045RH_m. \quad (4)$$

The slope is significant at the 99% confidence level. The differences in the range of RH_m and in the sampling for each period are the most likely causes of the differences in the correlations. Only 5% of the RH_m observations fall below 35% during the first period compared to almost 30% during the latter period. Conversely, nearly 25% of the RH_m values exceed 50% during 1993–94 while the frequency of $RH_m > 50\%$ is less than 3% during 1998–99.

The impact of the different ranges can be elucidated by combining the two datasets and averaging C_m for each 5% interval of RH_m . Figure 14c shows the means and standard errors of the mean for each interval. The contrail frequency increases with RH_m up to a plateau between 40% and 55% before dropping substantially at greater values of RH_m . This nonmonotonic behavior could arise for a variety of reasons such as the competition between contrails and cirrus clouds for the available moisture, co-occurrence of high RH_m with warm temperatures or limited air traffic, or by errors in RH_m . The last explanation is the easiest and can be supported to some extent by the relatively poor correlation between the NCEP and radiosonde values of RH (300 hPa) during the first period. Because of the problems associated with the radiosonde measurements and reporting practices at that time, however, it cannot be concluded that the NCEP data are any worse or better than the radiosonde data. Nor is it possible to fully assess the accuracy of the NCEP RH_m . The uncertainty in RH_m remains an open question.

The first explanation is more subtle. Clouds and persistent contrails only form in air that is supersaturated.

Contrails can develop and persist at levels of supersaturation with respect to ice that can be substantially lower than those required for the formation of natural cirrus clouds (Schumann 1996). As seen in Fig. 2, RH_m provides a rough estimate of the probability for supersaturated conditions. Thus, when it is relatively small, the frequency of large supersaturations (e.g., $R_h > 55\%$ in Fig. 2a) at flight level is less than that for the smaller supersaturations (e.g., R_h between 40% and 55% in Fig. 2a) that could sustain PCs. As RH_m rises, the frequencies of both large and small supersaturation increase along with PCs and natural cirrus clouds. As RH_m continues to grow, the rising frequency of larger supersaturations would eventually produce enough dense cirrus clouds such that contrail formation or detectability reaches a plateau and diminishes at even higher values of RH_m . This plateau is suggested in Fig. 2a by the nearly identical frequencies of R_h between 35% and 55% for the two highest ranges in $RH(300 \text{ hPa})$. Formation of observable contrails in these instances might be reduced because the additional cirrus clouds would form at the expense of the areas of small supersaturation or the contrails would form within the cirrus clouds (e.g., Poellot et al. 1999) and might not be observable if the cirrus cloud is optically thick.

The second possibility, that large values of RH_m are associated with warm temperatures or light air traffic was explored by examining each of the data points. Nearly 45% of the cases with $RH_m > 50\%$ occurred between June and September with only 36% occurring between January and May when the temperatures are optimal. Additionally, most of the values of $RH > 50\%$ are associated with sites outside the main airways. The mean fuel use for the months and sites with $RH_m > 50\%$ is 78% of the average value. Despite the warm temperatures and low fuel use, the average PC frequency was 0.119, a value 42% greater than the contrail fre-

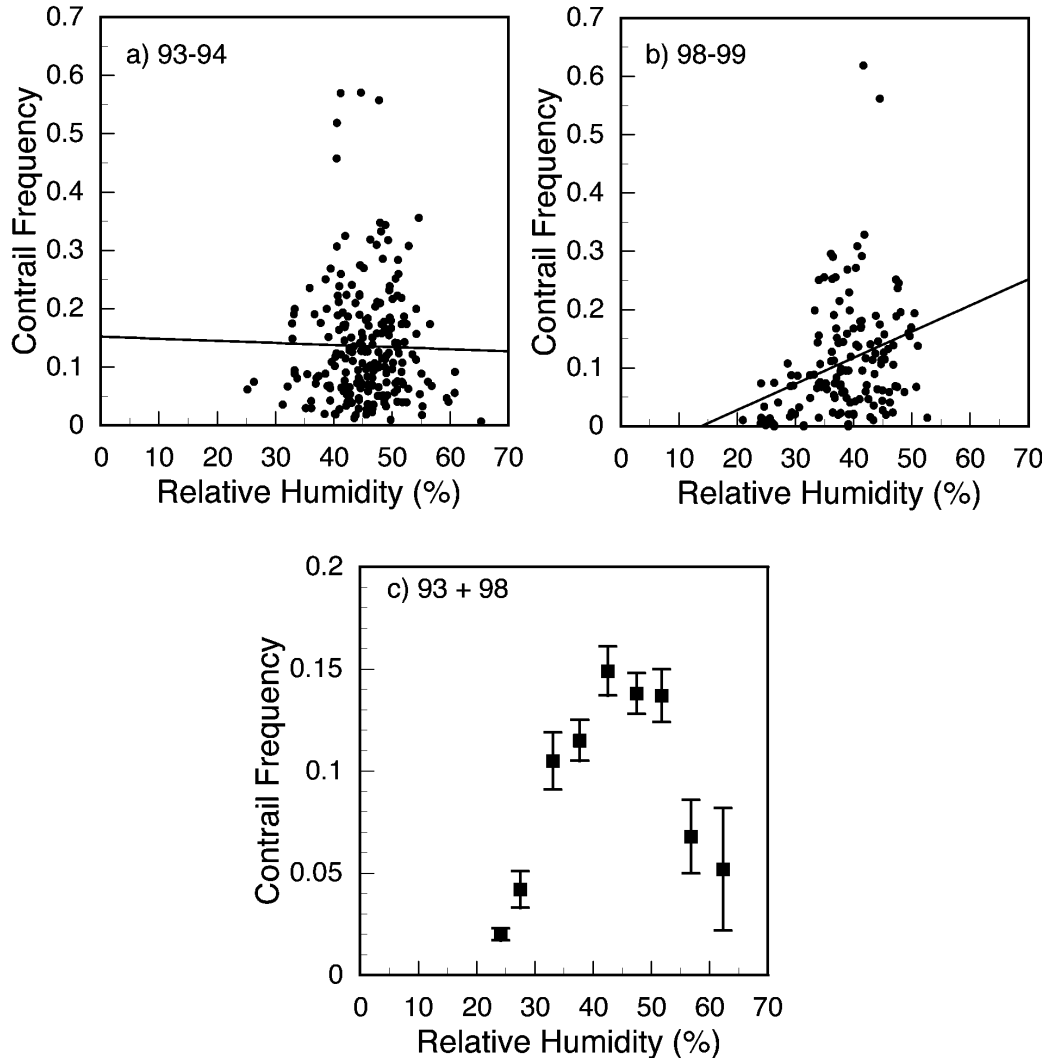


FIG. 14. Correlation of monthly mean contrail frequency and 300-hPa relative humidity during (a) 1993–94 and (b) 1998–99 and (c) variation of mean contrail frequency with 5 percentile means of RH_m .

quency computed with the equation in Fig. 11 using the mean fuel use ($95.6 \text{ million lb yr}^{-1}$) for the months and sites with $RH_m > 50\%$. The RH_m uncertainties and changing frequency distributions may have an impact on the nonmonotonic behavior, but it appears that the fuel use effect and seasonal (temperature) variability are the primary reasons for the drop in C_m at large values of RH_m .

It is clear from Fig. 13 and the above discussion that all three parameters studied thus far affect C_m . A multiple regression analysis using all of the data and each parameter yields

$$C_m = 2.089 + 0.00089f_m + 0.0031RH_m - (0.0095 \text{ K}^{-1})T_m. \quad (5)$$

The combination of parameters in (5) explains 45% of the variance in C_m , yielding a mean residual of 0.07.

Figure 15 shows the monthly means computed using (5) for each period. This simple model reproduces some features of the seasonal variations seen in Fig. 6b, but misses others. The maxima observed during late winter are significantly damped and the large interannual differences during March and April are missed with the model. The model variations during the second half of the year are in good agreement with those in Fig. 6b including the September 1998 minimum. The mean model value for 1998–99 is 0.133 compared to 0.135 for 1993–94.

Further improvement in the modeling of C_m would require the use of instantaneous values of each parameter at all levels where more contrails are formed instead using only the monthly means and values for temperature and humidity at 300 hPa. Additionally, using the actual flight paths through a given area at the relevant altitudes as in Duda et al. (2002) would be more ap-

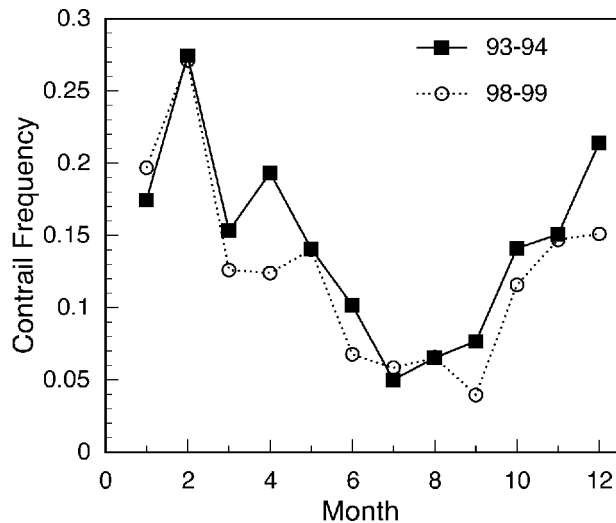


FIG. 15. Monthly mean contrail frequencies computed with (5) for monthly mean conditions.

propriate than using the average amount of fuel burned. Such datasets are not available for the time periods considered here. It should be stressed that the formulations in (1)–(5) are based on specific air traffic, temperature, and humidity datasets. As noted earlier, RH from radiosonde profiles can be significantly different from and will likely produce different results than the NCEP values. Other meteorological analysis products could also yield different results. Any use of the formulas should account for those differences.

d. Seasonal variability

Because these two periods represent extremes for RH (300 hPa), the more likely mean condition for PC frequency would be closer to the average for the two observation periods. The average maximum in late winter computed from Fig. 6b is nearly 4 times greater than the summertime minimum. Both theoretical (Sausen et al. 1998) and empirical (Mannstein et al. 2000) estimates of contrail coverage and satellite-derived contrail frequencies (DeGrand et al. 2000) yield a minimum during July, consistent with the broad summertime minimum seen here. Sausen et al. (1998) report a 400% increase in coverage from the July minimum to their April maximum, while DeGrand et al. (2000) find a 40% increase in frequency between July and their October maximum. Sausen et al. (1998) and DeGrand et al. (2000) find larger values for both coverage and frequency, respectively, during April than during January over the United States. The Sausen et al. (1998) mean coverage during January and October are the same, while Fig. 6b suggests that the contrail occurrence steadily increases between October and February. The preliminary results of Mannstein et al. (2000) and Palikonda et al. (2002) from 1993 and 2001 satellite data, respectively, are qualitatively consistent with the surface

observations. For example, during April, October, and December 1993, respective contrail coverage from Mannstein et al. (2000) was 0.020, 0.019, and 0.021, while the contrail frequencies for the 13 sites having measurements during all three months during 1993–94 were 0.188, 0.163, and 0.197.

Minnis et al. (1997) discussed several possible reasons for discrepancies with results based on satellite 11- μ m imagery alone (DeGrand et al. 2000). Another possibility is that, during winter, contrails over the United States might spread less and have lower optical depths than during other seasons (Ponater et al. 2002) making it more difficult to detect them in infrared imagery. In addition to the shortcomings in the surface observations note by Minnis et al. (1997), the differences between the theoretical results and the surface observations could arise from the highly uncertain humidities in the upper troposphere used in the model (Sausen et al. 1998).

To ensure that the results in Fig. 6 are representative of the seasonal variations over the CONUS, the months with the maximum values of PC for each time period for any site having observations during nine or more months are plotted in Fig. 16. The only trend suggested by this plot is the tendency for the maximum frequency to occur in the late spring or early winter in the more northern reaches of the domain. This tendency is qualitatively consistent with the results of DeGrand et al. (2000). It is likely that farther north, in Canada, the PC frequency would occur closer to July as found by DeGrand et al. (2000) because the mean 300-hPa temperatures for the northernmost sites are closer to the values seen in the central CONUS during the late winter and spring (see Fig. 21 of Minnis et al. 1997). The month with the most maxima is February followed by March, a result consistent with the maxima in contrail frequencies in Fig. 6.

Finally, using 10 yr of fish-eye camera data, Sassen (1997) found a maximum in contrail frequency during February over Salt Lake City, Utah, a result consistent with the February 1999 maximum over Hill AFB just north of Salt Lake City. From these results and the comparisons with Mannstein et al. (2000) and Palikonda et al. (2002), it is concluded that the annual cycle of PC frequency in Fig. 6b is representative of the United States as a whole. However, it is clear that the seasonal variation of PCs changes with latitude and the meteorological conditions at flight altitude. As suggested by Fig. 16, the frequency of PCs in any given month can differ significantly from the mean variation implied in Fig. 4b.

The identification of persistent contrails used in this study is subjective, as are all surface observations of clouds. Thus, some of the observed contrails may be more significant in terms of their climatological impact than others. As noted earlier, a number of other parameters must be measured to determine if a contrail of a particular size, depth, and lifetime is significant, a currently undefined measure. If it is assumed that a contrail

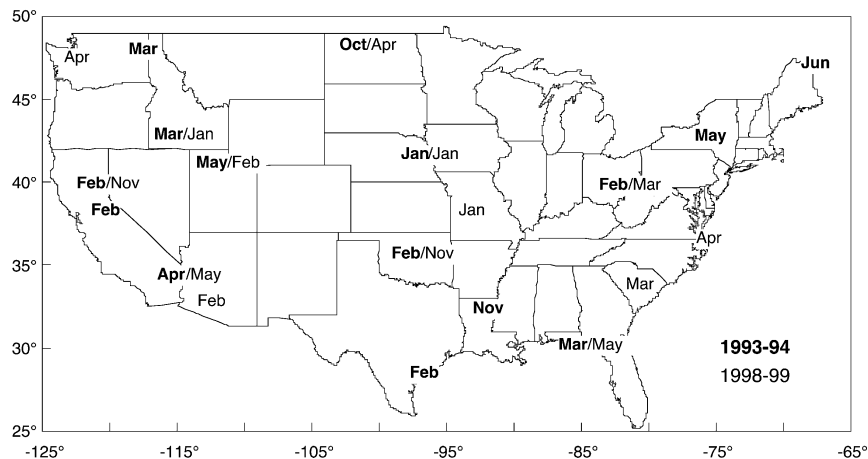


FIG. 16. Distribution of months with maximum contrail frequencies.

is climatologically significant when it can be identified in 1-km satellite imagery, then it is possible that many of the PCs identified here may not have spread sufficiently and lasted long enough to be climatologically significant. The reported frequencies would represent an overestimate of important contrails. Conversely, some of the larger, older contrails may not have been reported resulting in an underestimate of significant contrail frequencies. The results presented here do not necessarily represent the occurrence frequency of climatologically significant contrails, but they provide new information about the spatial and temporal distributions of conditions that produce a variety of persistent contrails. Moreover, they should be highly correlated with climatologically significant contrails because the spreading persistent contrails would constitute a subset of these observations.

5. Concluding remarks

As defined here, contrail frequency provides no information about the number of contrails observed each hour or their thickness and areal coverage. An increase in the number of flights may result in more contrails each hour rather than more hours with contrails. The number of hours when persistent contrails can form is limited by the amount of time that the formation conditions exist over a given site. Thus, the decreased frequency of persistent contrails during 1998–99 relative to 1993–94 resulting from the reduced humidity at flight levels might be accompanied by a greater number of contrails within each observation period. Such issues could probably be resolved with the analysis of high-resolution satellite data, which are required for the determination of contrail coverage and optical properties. The results presented here clearly demonstrate the substantial variability in the annual mean upper-tropospheric humidity over large areas and how it can affect mean contrail occurrences. It is important that climatologies

of contrail properties derived from satellite imagery and used to “tune” model simulations and prognostications should be based on data from multiple years to account for moisture variability.

When combined with the results from 1993–94, the 1998–99 data provide valuable independent information on the hourly, seasonal, and interannual variability of persistent contrails. The seasonal variations appear to be qualitatively consistent with preliminary satellite estimates of contrail coverage over the United States during the last decade. Model estimates of contrail effects on climate should be capable of reproducing, at some level, the variations over a wide range of temporal scales. Because the individual observations are available, it should also be possible to use the data to verify observed and modeled upper-tropospheric humidity. Predictions of potential contrail formation conditions can also be validated with the observations from both periods, especially when combined with information about flight times and altitudes. A more concerted and comprehensive observational effort is needed to quantify all of the parameters necessary for fully assessing the climatic impact of contrails.

Acknowledgments. This research was supported by the NASA Subsonic Assessment Program and the NASA Pathfinder Program and would not have been possible without the dedicated service of the many USAF weather observers. Thanks to David Duda and the two anonymous reviewers for their helpful comments and to Rabindra Palikonda for the ISCCP analyses.

APPENDIX

Observing Sites

Table A1 shows the locations and sampling for each station. Many of the regions were undersampled during

TABLE A1. Observing sites and monthly sampling.

| Station | Location | No. of months (1993–94) | No. of months (1998–99) |
|----------------------|-----------------|-------------------------|-------------------------|
| Barksdale, LA | 32.5°N, 93.7°W | 15 | 0 |
| Beale, CA | 39.1°N, 121.4°W | 14 | 12 |
| Cairns, AL | 31.3°N, 85.7°W | 8 | 4 |
| Cannon, NM | 34.4°N, 103.3°W | 0 | 5 |
| Edwards, CA | 34.9°N, 117.9°W | 12 | 10 |
| Eglin, FL | 30.5°N, 86.5°W | 10 | 10 |
| Fairchild, WA | 47.6°N, 117.7°W | 12 | 0 |
| Griffis, NY | 43.2°N, 75.4°W | 13 | 0 |
| Hill, UT | 41.1°N, 112.0°W | 12 | 11 |
| Kelly, TX | 28.9°N, 97.7°W | 13 | 0 |
| Langley, VA | 37.1°N, 76.4°W | 10 | 5 |
| Loring, ME | 46.9°N, 67.9°W | 12 | 0 |
| Luke, AZ | 33.5°N, 112.4°W | 8 | 10 |
| McClellan, CA | 38.7°N, 121.4°W | 13 | 6 |
| McChord, WA | 47.1°N, 122.5°W | 0 | 12 |
| Minot, ND | 48.4°N, 101.3°W | 13 | 10 |
| Mountain Home, ID | 43.1°N, 115.9°W | 13 | 8 |
| Offut, NE | 41.1°N, 95.9°W | 15 | 7 |
| Shaw, SC | 34.0°N, 80.5°W | 0 | 12 |
| Tinker, OK | 35.4°N, 97.4°W | 13 | 12 |
| Whiteman, MO | 38.7°N, 93.5°W | 16 | 1 |
| Wright-Patterson, OH | 39.8°N, 84.1°W | 12 | 9 |

the latter period. However, because the months that were sampled varied from region to region, the monthly sampling overall was relatively uniform except for February and March, which were significantly undersampled.

REFERENCES

- Appleman, H., 1953: The formation of exhaust condensation trails by jet aircraft. *Bull. Amer. Meteor. Soc.*, **34**, 14–20.
- Bakan, S., M. Betancour, V. Gayler, and H. Grassl, 1994: Contrail frequency over Europe from NOAA-satellite images. *Ann. Geophys.*, **12**, 962–968.
- Baughcum, S. L., 1996: Subsonic aircraft emission inventories. Atmospheric Effects of Aviation: First Report of the Subsonic Assessment Project, NASA RP-1385, 15–29.
- , L. Metwally, R. K. Seals, and D. J. Wuebbles, 1993: Emission scenarios development: Completed scenarios database. Atmospheric Effects of Stratospheric Aircraft: A Third Program, NASA RP-1313, 185–208.
- DeGrand, J. Q., A. M. Carleton, D. J. Travis, and P. J. Lamb, 2000: A satellite-based climatic description of jet aircraft contrails and associations with atmospheric conditions, 1977–79. *J. Appl. Meteor.*, **39**, 1434–1459.
- Duda, D. P., P. Minnis, P. K. Costulis, and R. Palikonda, 2002: An estimation of CONUS contrail frequency from RUC and flight track data. Preprints, *10th Conf. on Aviation, Range, and Aerospace Meteorology*, Portland, OR, Amer. Meteor. Soc., J70–J73.
- Elliott, W. P., R. J. Ross, and B. Schwartz, 1998: Effects on climate records of changes in National Weather Service humidity processing procedures. *J. Climate*, **11**, 2424–2436.
- Gaffen, D., 1993: Historical changes in radiosonde instruments and practices. WMO Instruments and Observing Methods Rep. 50, WMO/TD-No. 541, 123 pp.
- Hahn, C. J., S. G. Warren, J. London, R. M. Chervin, and R. Jenne, 1984: Atlas of simultaneous occurrence of different cloud types over land. NCAR Tech. Note NCAR/TN-241+STR, 213 pp.
- ICAO, 1998: International Civil Aviation Organization, Annual report on Civil Aviation. *ICAO J.*, **53**, 10–29.
- Kistler, R., and Coauthors, 2001: The NCEP–NCAR 50-Year Reanalysis: Monthly means CD-ROM and documentation. *Bull. Amer. Meteor. Soc.*, **82**, 247–267.
- Mannstein, H., R. Meyer, and P. Wendling, 1999: Operational detection of contrails from NOAA-AVHRR data. *Int. J. Remote Sens.*, **20**, 1641–1660.
- , —, P. Minnis, and R. Palikonda, 2000: Regional contrail coverage estimated from AVHRR data. *Proc. EUMETSAT Meteorological Satellite Data Users Conf. 2000*, Bologna, Italy, EUMETSAT, 578–585.
- Meerkötter, R., U. Schumann, D. R. Doelling, P. Minnis, T. Nakajima, and Y. Tsushima, 1999: Radiative forcing by contrails. *Ann. Geophys.*, **17**, 1070–1084.
- Miloshevich, L. M., H. Vömel, A. Pakkunen, A. J. Heymsfield, and S. J. Oltmans, 2001: Characterization and correction of relative humidity measurements from Vaisala RS80-A radiosondes at cold temperatures. *J. Atmos. Oceanic Technol.*, **18**, 135–156.
- Minnis, P., J. K. Ayers, and S. P. Weaver, 1997: Surface-based observations of contrail occurrence frequency over the U.S., April 1993–April 1994. NASA RP-1404, 81 pp. [Available online at <http://techreports.larc.nasa.gov/ltrs/PDF/1997/NASA-97-rp1404.pdf>]
- , D. F. Young, L. Nguyen, D. P. Garber, W. L. Smith Jr., and R. Palikonda, 1998: Transformation of contrails into cirrus during SUCCESS. *Geophys. Res. Lett.*, **25**, 1157–1160.
- , U. Schumann, D. R. Doelling, K. M. Gierens, and D. W. Fahey, 1999: Global distribution of contrail radiative forcing. *Geophys. Res. Lett.*, **26**, 1853–1856.
- , L. Nguyen, D. P. Duda, and R. Palikonda, 2002: Spreading of isolated contrails during the 2001 air traffic shutdown. Preprints, *10th Conf. on Aviation, Range, and Aerospace Meteorology*, Portland, OR, Amer. Meteor. Soc., 33–36.
- Palikonda, R., P. Minnis, P. K. Costulis, and D. P. Duda, 2002: Contrail climatology over the USA from MODIS and AVHRR data. Preprints, *10th Conf. on Aviation, Range, and Aerospace Meteorology*, Portland, OR, Amer. Meteor. Soc., J9–J12.
- Penner, J. E., D. H. Lister, D. J. Griggs, D. J. Dokken, and M. McFarland, Eds., 1999: *Aviation and the Global Atmosphere*. Cambridge University Press, 373 pp.
- Poellot, M. R., W. P. Arnott, and J. Hallett, 1999: In situ observations of contrail microphysics and implications for their radiative impact. *J. Geophys. Res.*, **104**, 12 977–12 984.
- Ponater, M., S. Marquart, and R. Sausen, 2002: Contrails in a comprehensive global climate model: Parameterization and radiative forcing results. *J. Geophys. Res.*, **107**, 4164, doi:10.1029/2001JD0000429.
- Rossov, W. B., and R. A. Schiffer, 1999: Advances in understanding clouds from ISCCP. *Bull. Amer. Meteor. Soc.*, **80**, 2261–2287.
- Sassen, K., 1997: Contrail-cirrus and their potential for regional climate change. *Bull. Amer. Meteor. Soc.*, **78**, 1885–1904.
- Sausen, R., K. Gierens, M. Ponater, and U. Schumann, 1998: A diagnostic study of the global coverage by contrails. Part I: Present day climate. *Theor. Appl. Climatol.*, **61**, 127–141.
- Schumann, U., 1996: On conditions for contrail formation from aircraft exhausts. *Meteor. Z.*, **5**, 4–23.
- Soden, B. J., and J. R. Lanzante, 1996: An assessment of satellite and radiosonde climatologies of upper-tropospheric water vapor. *J. Climate*, **9**, 1235–1250.
- Tian, L., and J. Curry, 1989: Cloud overlap statistics. *J. Geophys. Res.*, **94**, 9925–9935.